ISPEC Fen Bilimleri Enstitüsü Dergisi, 4(1):60-71, 2025
ISPEC Journal of Science Institute, 4(1):60-71, 2025
DOI: https://doi.org/10.5281/zenodo.15783566

Alternative Approach to The Line Integral Representations of Fringe Waves

Hüsnü Deniz BASDEMİR[1*]

[1] Sivas University of Science and Technology, Faculty of Engineering and Naturel Sciences & Faculty of Aviation and Space Sciences, Sivas
Sorumlu Yazar (Corresponding author): denizbasdemir@gmail.com

Abstract
In this paper, the line integral representations of fringe field expressions are derived analytically and generalized using the unit vectors of the related edge contours. The derived expressions are applied to the perfectly electric conducting (PEC) parabolic reflector geometry to investigate the exact diffracted fields.

Research Article

Article History
Received : 28.05.2025
Accepted: 30.06.2025

Keywords
Fringe Fields,
Parabolic Reflector,
Diffraction

1. Introduction

Young first proposed the physical meaning of the scattered fields from a knife edge by superpositioning the incident and edge-diffracted fields (Rubinowicz, 1957). Although his valuable idea was allowed to show the interference characteristic of the scattered fields, he could not base it on the mathematical basis of this explanation. Therefore, this proposal was dominated by the Fresnel's theory of diffraction. Later on, Maggi and Rubinowitz independently derived the mathematical expressions, which are realized in Young's idea using Kirchoff's integral formula (Maggi, 1888; Rubinowicz, 1917). The obtained line integrals are the reduction forms of the surface integrals to the line integrals, and the evaluation of these integrals directly gives rise to the edge-diffracted fields. This theory leads to investigating the diffracted fields independently from the scattered fields. However, Ganci's works on the half plane showed that the solution of the Maggi-Rubinowitz (boundary diffraction wave, BDW) gives an approximate solution like physical optics (PO) (Ganci, 1996; Ganci, 1995). PO is a high-frequency asymptotic technique, and it is widely used in the literature to investigate scattering problems (Guan et al., 2011; Hamel et al., 2012; Huang et al., 2011; Lee et al., 2008; Letrou and Boag, 2012; Roudstein and Boag, 2011; Wu et al., 2011). Although it is accurate for analyzing the scattering from large metallic objects, PO gives wrong diffracted fields at the edges. The second defeat of the PO is the definition of surface currents. The definition of the surface currents doesn't include the contributions of the shadow parts. The physical theory of diffraction (PTD) is one of the well-known integral-based techniques suggested by Ufimtsev in the 1950s (Ufimtsev, 2006). PTD method corrects the defeats of the PO by defining additional correction currents. These currents are called fringe currents.

Ufimtsev also improved this theory by reducing his surface integrals to reduce the edge point contributions, but he did it indirectly, using heuristic considerations (Ufimtsev, 1962). Mitzner and Michaeli also independently used this surface to edge reduction technique (Mitzner, 1974; Michaeli, 1984). The result of Mitzner's work was formulated in terms of the incremental length diffraction coefficients (ILDC), and Michaeli's work was formulated in terms of the equivalent edge currents (EEC) for wedge like solutions. Both approaches were compared by Knott (Knott, 1985). Michaeli's expressions are finite for all directions of incidence and observation for edges. The observation point is described in the oblique incidence with two different angles. The first one, β is related to the edge contour, and the second one, φ is associated with the plane of the perpendicular incidence. The scattering angle β was taken differently than the incident angle by Michaeli for the oblique incidence. Hence, the equivalent edge currents were improved for the observation points out of the Keller's cone. The angle β is the function of the integral variable, but he did not modify the φ angle. According to Michaeli's equivalent edge current method, the angle of φ is not a function of the integration variable. However, the φ angle takes different values at the discontinuity of the edges than the values on the edges. Because of this, the method gives wrong diffracted fields at the corners. Umul has overcome this corner problem by defining the exact form of the equivalent edge currents using the axioms of the modified theory of physical optics (MTPO) (Umul 2009; Umul 2008a). This study will obtain and generalize a rigorous form of the fringe field expressions using the unit vectors. The obtained expressions will be applied to the parabolic reflector geometry, which has the perfectly electric conducting (PEC) boundary condition and is fed by the H-polarized magnetic line source. The method, which is based on the MTPO axioms, will be applied. Many researchers have studied curved surface diffraction. The scattering of the electromagnetic fields from the curved surfaces was studied by Büyükaksoy and Uzgören (Bueyuekaksoy and Uzgoeren, 1987) and Akduman and Büyükaksoy (Akduman and Büyükaksoy, 1995). Umul investigated the scattering of a line source from a cylindrical parabolic impedance reflector (Umul, 2008b). Yalcin investigated scattering from a cylindrical reflector fed by an offset electrical line source (Yalçin, 2007).

The time factor of $exp(j\omega t)$ is assumed and suppressed throughout the paper where ω is the angular frequency.

2. Derivation of the Fringe Fields

First, the PO diffraction field will be obtained for the half plane problem. The geometry of the half plane is given in the Fig. 1. The half plane is lying on the surface $\{x \in [0,\infty], y = 0, z \in [-\infty,\infty]\}$. P and Q are the arbitrary observation and integration points, respectively.

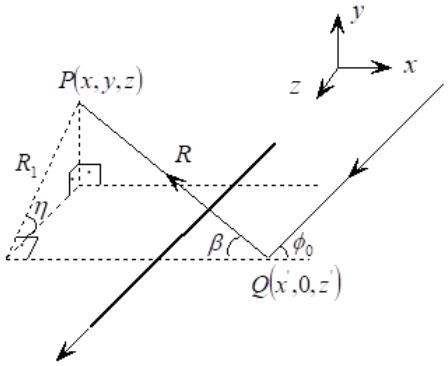

Figure 1. The geometry of the half plane

The incident field can be given as

$$\vec{H}_i = \vec{e}_z H_0 e^{jk(x\cos\varphi_0 + y\sin\varphi_0)} \qquad (1)$$

for the magnetic field polarization. PO current is defined as

$$\vec{J}_{PO} = 2\vec{n} \times \vec{H}_i\big|_s \qquad (2)$$

where $\vec{n}$ is the unit normal vector of the half plane and equal to $\vec{e}_y$. Magnetic vector potential is written as

$$\vec{A} = \frac{\mu_0}{4\pi} \iint_{s'} \vec{J}_{PO} \frac{e^{-jkR}}{R} dS'. \qquad (3)$$

The connection between the magnetic vector potential and the scattered magnetic field can be satisfied by

$$\vec{H} = \frac{1}{\mu_0} \nabla \times \vec{A} \quad . \qquad (4)$$

PO current is written as

$$\vec{J}_{PO}\big|_{s'} = \vec{e}_x 2H_0 e^{jkx'\cos\varphi_0} \qquad (5)$$

with using the Eq. (1) and Eq. (2). Diffraction integral can be composed as

$$\vec{H} = \frac{H_0}{2\pi} \int_{z'=-\infty}^{\infty} \int_{x'=0}^{\infty} e^{jkx'\cos\varphi_0} \nabla \times \left(\vec{e}_x \frac{e^{-jkR}}{R}\right) dx'dz' \qquad (6)$$

with using the Eq. (3), Eq. (4), and Eq. (5) where R is the ray path and equal to $\left[(x-x')^2 + y^2 + (z-z')^2\right]^{1/2}$. The curl operation in the Eq. (6) is given as

$$\nabla \times \left(\vec{e}_x \frac{e^{-jkR}}{R}\right) = -\vec{e}_y \frac{jk(z-z')}{R} \frac{e^{-jkR}}{R} + \vec{e}_z jk \frac{y}{R} \frac{e^{-jkR}}{R} \qquad (7a)$$

and from the Fig. 1 Eq. (7a) is decomposed as

$$\nabla \times \left(\vec{e}_x \frac{e^{-jkR}}{R}\right) = -\vec{e}_y jk\cos\eta\sin\beta \frac{e^{-jkR}}{R} + \vec{e}_z jk\sin\eta\sin\beta \frac{e^{-jkR}}{R} \qquad (7b)$$

where $\cos\eta = \frac{z-z'}{R_1}$, $\sin\beta = \frac{R_1}{R}$ and $\sin\eta = \frac{y}{R_1}$ respectively. Hence, Eq. (6) is decomposed as

$$\vec{H} = \frac{H_0}{2\pi} \int_{z'=-\infty}^{\infty} \int_{x'=0}^{\infty} e^{jkx'\cos\varphi_0} \left(-\vec{e}_y jk\cos\eta\sin\beta + \vec{e}_z \sin\eta\sin\beta\right) \frac{e^{-jkR}}{R} dx'dz' \qquad (8)$$

according to the Eq. (7b). x' part of the Eq. (8) can be taken using the well-known edge point technique. The edge point technique is given

$$\int_a^{\infty} f(x) e^{-jkg(x)} dx = \frac{1}{jk} f(a) \frac{1}{g'(a)} e^{-jkg(a)}. \qquad (9)$$

The phase function of the diffraction integral is written as

$$\psi = x'\cos\varphi_0 - R \qquad (10)$$

where the first derivative ψ' is equal to $\cos\varphi_0 + \frac{x-x'}{R}$. The amplitude function is written as

$$f(x) = \frac{\cos\eta\sin\beta}{R}. \qquad (11)$$

At the $x' = 0$ point the phase function and its derivative takes the form as

$$\psi = R_e \qquad (12a)$$

and

$$\psi' = cos\varphi_0 - cos\beta_e \qquad (12b)$$

where R_e is the ray path at the $x' = 0$ and equal to $\left[\rho^2 + (z - z')^2\right]^{1/2}$. The amplitude function takes the form as

$$f(x' = 0) = \frac{cos\,\eta sin\beta_e}{R_e}. \qquad (13)$$

Hence, the diffraction integral takes the form as

$$\vec{H} = \frac{H_0}{2\pi}\int_{z'=-\infty}^{\infty}\left(-\vec{e}_y\, cos\,\eta\, sin\beta_e + \vec{e}_z\, sin\,\eta\, sin\beta_e\right)\ \frac{1}{cos\varphi_0 - cos\beta_e}\frac{e^{-jkR_e}}{R_e}\,dz' \qquad (14)$$

using Eq. (12a), (12b), and Eq. (13). The stationary phase method can be used to evaluate the z' part of the diffraction integral. The phase function of the integral is written as

$$\psi = R_e \qquad (15)$$

where the first derivative of the phase function is equal to $-\frac{z-z'}{R_e}$. The stationary phase point can be found by equating the first derivative of the phase function to zero. Then, the stationary phase point is found as

$$z_s = z. \qquad (16)$$

At the stationary phase points η and β_e values are equal to $\frac{\pi}{2}$ and $\pi - \varphi$ respectively. The second derivative of the phase function is written as

$$\psi'' = -\frac{-R_e^2 + (z - z')}{R_e^3} \qquad (17)$$

and it is equal to $\frac{1}{R_e}$ at the stationary phase point. The amplitude function can be written as

$$f(z' = z) = \frac{sin\varphi_0}{cos\varphi_0 + cos\,\varphi}\frac{1}{\rho} \qquad (18)$$

at the stationary phase point. Hence, PO diffracted magnetic field is written as

$$\vec{H} = \vec{e}_z \frac{H_0}{\sqrt{2\pi}} e^{-j\frac{\pi}{4}} \frac{sin\,\varphi}{cos\,\varphi + cos\varphi_0}\frac{e^{-jk\rho}}{\sqrt{k\rho}}. \qquad (19)$$

The exact diffracted field from the half plane is written as

$$\vec{H}_d = -\vec{e}_z H_0 \frac{e^{-j\frac{\pi}{4}}}{2\sqrt{2\pi}}\left(\frac{1}{cos\frac{\varphi - \varphi_0}{2}} + \frac{1}{cos\frac{\varphi + \varphi_0}{2}}\right)\frac{e^{-jk\rho}}{\sqrt{k\rho}}. \qquad (20)$$

Equation (20) is rearranged as

$$\vec{H}_d = -\vec{e}_z H_0 \frac{e^{-j\frac{\pi}{4}}}{\sqrt{2\pi}} \frac{2\,cos\frac{\varphi}{2} cos\frac{\varphi_0}{2}}{cos\,\varphi + cos\varphi_0}\frac{e^{-jk\rho}}{\sqrt{k\rho}}. \qquad (21)$$

The difference between the exact diffracted field and the PO diffracted field can be found as

$$\vec{H}_f = -\vec{e}_z \frac{e^{-j\frac{\pi}{4}}}{\sqrt{2\pi}} \frac{2\,cos\frac{\varphi}{2} cos\frac{\varphi_0}{2} - sin\,\varphi}{cos\,\varphi + cos\varphi_0}\frac{e^{-jk\rho}}{\sqrt{k\rho}} \qquad (22)$$

where $\vec{H}_f$ is found to be a fringe field. A new coordinate system and other related angles are given in Fig. 2 to generalize the magnetic fringe current.

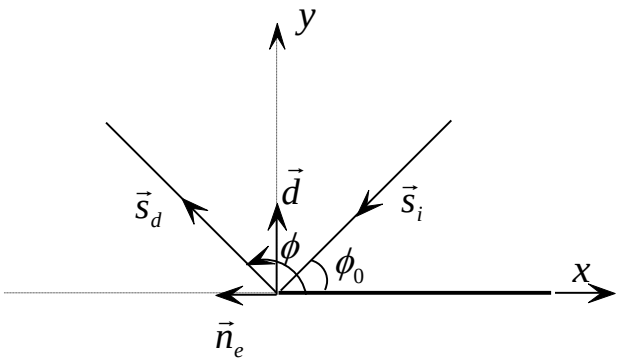

Figure 2. The geometry of the related angles

The following relations are written

$$cos\,\varphi = -\vec{s}_d \cdot \vec{n}_e, sin\,\varphi = \vec{s}_d \cdot \vec{d}, \qquad (23a)$$

$$cos\varphi_0 = \vec{s}_i \cdot \vec{n}_e \qquad (23b)$$

and

$$cos\,\frac{\varphi}{2} = \frac{1}{\sqrt{2}}\sqrt{1 - \vec{s}_d \cdot \vec{n}_e} \qquad (24a)$$

$$cos\,\frac{\varphi_0}{2} = \frac{1}{\sqrt{2}}\sqrt{1 + \vec{s}_i \cdot \vec{n}_e} \qquad (24b)$$

from the kinds of direction vectors where $\vec{n}_e$ is the vector that is outwards from the edge in the direction of the tangent of the surface. The expression of the fringe field is found as

$$\vec{H}_f = -\vec{e}_z \frac{e^{-j\frac{\pi}{4}}}{\sqrt{2\pi}} \frac{\sqrt{1+\vec{s}_i\cdot\vec{n}_e}\sqrt{1-\vec{s}_d\cdot\vec{n}_e} - \vec{s}_d.\vec{d}}{(\vec{s}_i - \vec{s}_d)\cdot\vec{n}_e} \frac{e^{-jk\rho}}{\sqrt{k\rho}} \qquad (25)$$

in terms of the direction vector. Hence, generalized magnetic fringe fields integral expression is defined as

$$\vec{H}_f = -\vec{e}_z \frac{1}{2\pi} \int_C H_i(Q_e) \frac{\sqrt{1+\vec{s}_i\cdot\vec{n}_e}\sqrt{1-\vec{s}_d\cdot\vec{n}_e} - \vec{s}_d\cdot\vec{d}}{(\vec{s}_i - \vec{s}_d)\cdot\vec{n}_e} \frac{e^{-jkR_e}}{R_e} dl \qquad (26)$$

3. Application

The geometry of the problem is presented in Fig. 3 where φ' is the angle of incidence, ρ is the distance between the source and observation points, ρ' is the distance between the source and the reflector, $\vec{n}$ is the unit normal vector, R is the ray path and P, Q are the observation and reflection points, respectively. The angle between $\vec{n}$ and ρ' is equal to $\frac{\varphi'}{2}$. f is the focal length of the PEC reflector. The PEC cylindrical reflector is lying between the angles $-\varphi_0$ and φ_0.

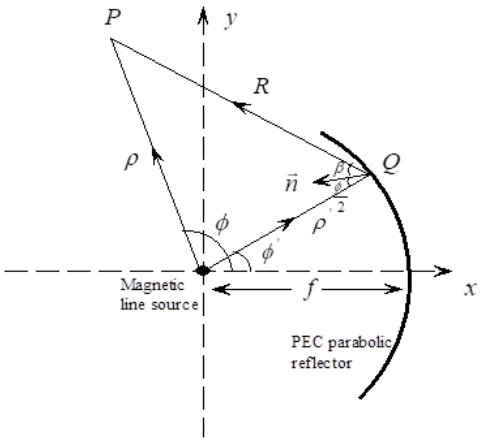

Figure 3. The geometry of the parabolic reflector, which is illuminated by the magnetic line source

As can be seen from Fig. 3, the parabolic reflector is fed by the magnetic line source, which is defined as

$$\vec{H}_i = \vec{e}_z I_m \frac{e^{-jk\rho}}{\sqrt{k\rho}} \qquad (27)$$

where I_m is the complex amplitude factor. PO electric current can be written directly

$$\vec{J}_{PO} = 2\left(cos\frac{\varphi'}{2}\vec{e}_\varphi + sin\frac{\varphi'}{2}\vec{e}_\rho\right) I_m \frac{e^{-jk\rho'}}{\sqrt{k\rho'}} \qquad (28)$$

where $\vec{n}$ is the unit normal vector which is defined in the Eq. (2) and equal to $-cos\frac{\varphi'}{2}\vec{e}_\rho + sin\frac{\varphi'}{2}\vec{e}_\varphi$ for the problem geometry. The scattered magnetic field is written as

$$\vec{H}_{PO} = \frac{I_m}{2\pi}\iint_{S'} \nabla \times \left(\vec{e}_\varphi cos\frac{\varphi'}{2}\frac{e^{-jkR}}{R} + \vec{e}_\rho sin\frac{\varphi'}{2}\frac{e^{-jkR}}{R}\right)\frac{e^{-jk\rho'}}{\sqrt{k\rho'}} dS' \qquad (29)$$

from expressions of the Eq. (3), (4), and Eq. (27). R is the ray path and equal to $\left[\rho^2 + \rho'^2 - 2\rho\rho' cos(\varphi - \varphi') + (z - z')^2\right]^{1/2}$ where ρ' is equal to $\frac{f}{cos^2\frac{\varphi}{2}}$. The curl operation of the Eq. (29) is written as

$$\frac{1}{\rho}\left(\vec{e}_z\left(cos\frac{\varphi'}{2}\frac{e^{-jkR}}{R} - cos\frac{\varphi'}{2}jk\frac{e^{-jkR}}{R}\frac{\partial R}{\partial\rho} + sin\frac{\varphi'}{2}jk\frac{e^{-jkR}}{R}\frac{\partial R}{\partial\varphi}\right)\right) \qquad (30)$$

where the derivatives of the ray path according to the ρ and φ are equal to $\frac{\rho - \rho' cos(\varphi - \varphi')}{R}$ and $\frac{\rho\rho' sin(\varphi - \varphi')}{R}$ respectively. The angle equalities of the derivative values can be written as

$$\frac{\partial R}{\partial\rho} = cos\left(\varphi - \frac{\varphi'}{2} + \beta\right) \qquad (31a)$$

and

$$\frac{\partial R}{\partial\varphi} = sin\left(\varphi - \frac{\varphi'}{2} + \beta\right) \qquad (31b)$$

from Fig. 3. The angle equalities are inserted into Eq. (30), and the rearranged form of Eq. (30) is written as

$$\vec{e}_z \left\{ \frac{e^{-jkR}}{R} \left(\frac{1}{\rho} cos \frac{\varphi'}{2} + jk\, cos(\varphi - \varphi' + \beta) \right) \right\} \quad (32)$$

to be the end of the curl operation. The Eq. (29) is rewritten as

$$\vec{H}_{PO} = \vec{e}_z \frac{I_m}{2\pi} \int_{z'=-\infty}^{\infty} \int_{\varphi'=-\varphi_0}^{\varphi_0} \frac{e^{-jk\rho'}}{\sqrt{k\rho'}} \left(\frac{1}{\rho} cos \frac{\varphi'}{2} + jk\, cos(\varphi - \varphi' + \varphi) \right) \frac{e^{-jkR}}{R} \rho' d\varphi' dz' \quad (33)$$

with using Eq. (29) and Eq. (32). The z'part of the integral can be eliminated

$$\int_c e^{-jkR_1 ch\alpha} d\alpha = \frac{\pi}{j} H_0^{(2)}(kR_1) \quad (34)$$

where $z - z' = R_1 sh\alpha$ and $R = [R_1^2 + (z - z')^2]^{1/2}$. Hence, Eq. (33) is written as

$$\vec{H}_{PO} = \vec{e}_z \frac{I_m}{2j} \int_{\varphi'=-\varphi_0}^{\varphi_0} \frac{e^{-jk\rho'}}{\sqrt{k\rho'}} \left(\frac{1}{\rho} cos \frac{\varphi'}{2} + jk\, cos(\varphi - \varphi' + \beta) \right) H_0^{(2)}(kR_1) \rho' d\varphi' \quad (35)$$

for Eq. (34). The effect of the edges of the parabolic reflector can be found by applying the fringe field expression. The geometry of the diffracted field is given in the Fig. 4.

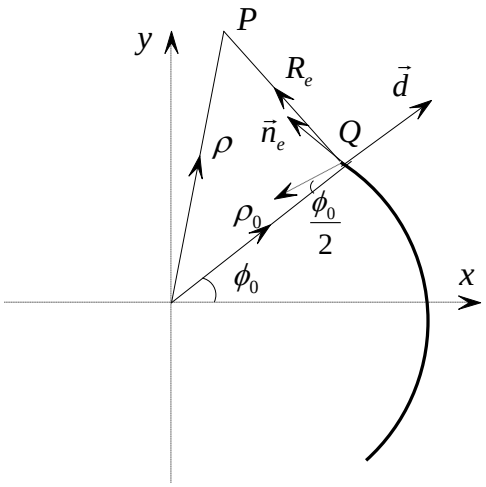

Figure 4. The geometry of the diffracted field

The related expressions are defined as

$$\vec{s}_i = \vec{d}\, cos \frac{\varphi_0}{2} + \vec{n}_e\, sin \frac{\varphi_0}{2} \quad (36)$$

and

$$\vec{s}_d = \vec{n}_e\, cos\, \beta + \vec{d}\, sin\, \beta\, sin\, \eta \quad (37)$$

where $\vec{d} = \vec{e}_\rho$and $\vec{n}_e = \vec{e}_\varphi$ for the upper edge. When the Eq. (36) and Eq. (37) are inserted to the Eq. (26), the fringe field expression is written as

$$\vec{H}_f^u = -\vec{e}_z \frac{1}{2\pi}$$

$$\int_{z'=-\infty}^{\infty} I_m \frac{e^{-jk\rho_0}}{\sqrt{k\rho_0}} \frac{\sqrt{1 + sin\frac{\varphi_0}{2}} \sqrt{1 - cos\, \beta} - sin\, \beta\, sin\, \eta}{sin\frac{\varphi_0}{2} - cos\, \beta}$$

$$\frac{e^{-jkR_e}}{R_e} dz^{'} \qquad (38)$$

where R_e is the ray path and equal to $[\rho^2 + \rho_0^2 - 2\rho\rho_0\, cos(\varphi - \varphi_0) + (z - z^{'})^2]^{1/2}$. The phase function is written as

$$\psi = R_e \qquad (39)$$

where the first derivative of the phase function is equal to $\psi^{'} = -\frac{z-z^{'}}{R_e}$. The stationary phase point can be found by equating the first derivative of the phase function to zero. Hence, the stationary phase point $z_s^{'}$ is equal to z. The second derivative of the phase function can be written as

$$\psi_s^{''} = \frac{1}{R_{es}} \qquad (40)$$

at the stationary phase point where R_{es} is equal to $[\rho^2 + \rho_0^2 - 2\rho\rho_0\, cos(\varphi - \varphi_0)]^{1/2}$. The amplitude function is written as

$$f(z_s^{'} = z) = \frac{\sqrt{1+sin\frac{\varphi_0}{2}}\sqrt{1-cos\,\beta} - sin\beta_s\, sin\eta_s}{sin\frac{\varphi_0}{2} - cos\beta_s} \frac{1}{R_{es}} \qquad (41)$$

at the stationary phase point. Hence, Eq. (38) can be rewritten as

$$\vec{H}_f^u = -\vec{e}_z \frac{I_m}{\sqrt{2\pi}} \frac{e^{-jk\rho_0}}{\sqrt{k\rho_0}}$$

$$e^{-j\frac{\pi}{4}} \frac{\sqrt{1+sin\frac{\varphi_0}{2}}\sqrt{1-cos\beta_s} - sin\beta_s\, sin\eta_s}{sin\frac{\varphi_0}{2} + cos\beta_s} \frac{e^{-jkR_{es}}}{\sqrt{kR_{es}}} \qquad (42)$$

where the β_s and η_s is equal to $\pi - \varphi$ and $\frac{\pi}{2}$, respectively. The related expressions for the lower edge of the PEC cylindrical reflector are defined as

$$\vec{s}_i = \vec{d}\, cos\frac{\varphi_0}{2} + \vec{n}_e\, sin\frac{\varphi_0}{2} \qquad (43)$$

and

$$\vec{s}_d = \vec{n}_e\, cos\,\beta + \vec{d}\, sin\,\beta\, sin\,\eta \qquad (44)$$

where $\vec{d}$ and $\vec{n}_e$ is equal to $\vec{e}_\rho$ and $-\vec{e}_\varphi$ respectively. The Eq. (26) is written as

$$\vec{H}_f^l = \vec{e}_z \frac{I_m}{2\pi} \frac{e^{-jk\rho_0}}{\sqrt{k\rho_0}}$$

$$\int_{z=-\infty}^{\infty} \frac{\sqrt{1+sin\frac{\varphi_0}{2}}\sqrt{1-cos\,\beta} - sin\,\beta\, sin\,\eta}{sin\frac{\varphi_0}{2} - cos\,\beta} \frac{e^{-jkR_e}}{R_e} dz \qquad (45)$$

for the lower edge where R_e is equal to $[\rho^2 + \rho_0^2 - 2\rho\rho_0\, cos(\varphi + \varphi_0) + (z - z^{'})^2]^{1/2}$. The phase function of the Eq. (45) is written as

$$\psi = R_e \qquad (46)$$

and its first derivative ψ' is equal to $-\frac{z-z'}{R_e}$. The stationary phase point can be found as $z_s' = z$ with equating the first derivative of the phase function to zero. The second derivative of the phase function is written as

$$\psi_s'' = \frac{1}{R_{es}} \qquad (47)$$

at the stationary phase point and R_{es} is equal to $[\rho^2 + \rho_0^2 - 2\rho\rho_0\, cos(\varphi + \varphi_0)]^{1/2}$. The value of the amplitude function is written as

$$f(z_s' = z) = \frac{\sqrt{1+sin\frac{\varphi_0}{2}}\sqrt{1-cos\beta_s}-sin\beta_s\, sin\eta_s}{sin\frac{\varphi_0}{2}-cos\beta_s}\frac{1}{R_{es}} \qquad (48)$$

at the stationary phase point and the values of the angles β_s, η_s are equal to $\pi - \varphi$ and $\frac{\pi}{2}$, respectively. Hence, Eq. (45) is rewritten as

$$\vec{H}_f^l = -\vec{e}_z \frac{I_m}{\sqrt{2\pi}} \frac{e^{-jk\rho_0}}{\sqrt{k\rho_0}} e^{-j\frac{\pi}{4}} \frac{\sqrt{1+sin\frac{\varphi_0}{2}}\sqrt{1-cos\beta_s}-sin\beta_s}{sin\frac{\varphi_0}{2}-cos\beta_s} \frac{e^{-jkR_{es}}}{\sqrt{kR_{es}}}. \qquad (49)$$

The exact diffracted field can be found as

$$\vec{H}_E = \vec{H}_{PO} + \vec{H}_f^u + \vec{H}_f^l \qquad (50)$$

with adding the contributions of the fringe fields to the PO diffracted field.

4. Numerical Analysis

In this analysis, the exact diffracted fields, fringe fields, and diffracted PO fields will be investigated. The observation distance is taken reasonably from the scatterer to investigate the far field radiation. The observation distance will be taken as 7λ, where λ is the wavelength. The focal length f will be taken as 2λ. The parabolic reflector will be positioned between the angles $-\varphi_0$ andφ_0.

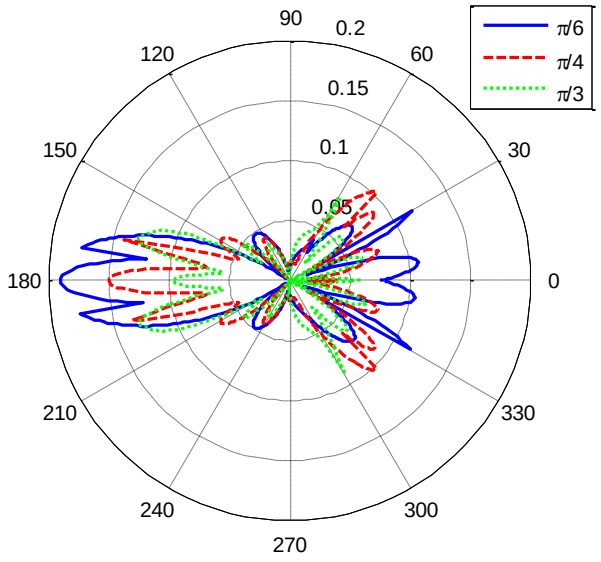

Figure 5. Exact diffracted fields

Figure 5 shows the exact diffracted fields from the edges of the parabolic reflector, which is given in Eq. (49) for different incident angles. The amplitude values of the diffracted fields are significant in the reflection region. The main beams can be observed between the angles 150˚ and 210˚. The maximum radiation is observed at 180˚. The fields' amplitudes take the minimum values at 90˚ and 270˚. The effect of the incident angleφ_0 can be seen directly from Fig. 5. The diffracted fields' amplitudes decrease in the reflection region when the incident angle increases.

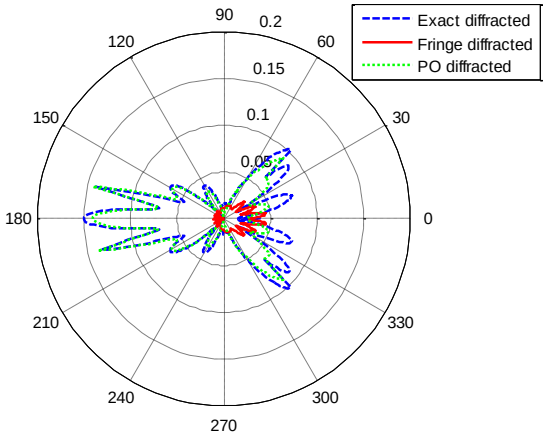

Figure 6. PO, fringe, and exact diffracted fields for $\varphi_0 = \frac{\pi}{4}$

Figure 6 shows the exact, fringe and PO diffracted fields. PO diffracted field in perfect harmony with the exact diffracted field except for the reflection boundaries, which are the angles 45˚ and 315˚, respectively. PO and exact diffracted fields take maximum amplitude values at 180˚. Although the PO diffracted field's amplitude goes to zero at 90˚ and 270˚, exact diffracted fields take different amplitude values at that angle. The fringe diffracted fields' amplitude takes the major values between the reflection regions. The minor lobes are observed between the angles 90˚ and 270˚. The fringe diffracted fields fix the defeats of the PO diffracted fields in reflection and shadow boundaries and reflection and shadow regions.

4. Conclusions

In this study, scattering surface integrals were reduced to the line integrals to investigate the exact diffracted fields. In addition, this formulation was generalized for various diffraction applications. This formulation is based on the MTPO axioms. In contrast to the other approaches, this derived expression is based on the MTPO axioms, and the scattering angle is variable at the corners and the edges. This is the main advantage of this approach. This new formulation was applied to the PEC cylindrical parabolic reflector geometry, which was fed by the H-polarized line source. The PO diffracted fields were found. Fringe field expressions were derived. The asymptotic evaluations of the diffraction integrals were yielding the fringe fields. The fringe fields were used to fix the PO diffracted fields, and the exact diffracted fields were obtained. The PO, fringe, and exact diffracted fields were analyzed numerically. The exact diffracted fields were investigated numerically for different incident angles. It is observed that the results are in harmony with the theory.

References

Akduman, I., Büyükaksoy, A., 1995. Asymptotic expressions for the surface currents induced on a cylindrically curved impedance strip. *IEEE Trans Antennas Propag*, 43.

Büyükaksoy, A., Uzgören, G., 1987. High-frequency scattering from the impedance discontinuity on a cylındrically curved surface. *IEEE Trans Antennas Propag*, AP-35.

Ganci, S., 1995. A general scalar solution for the half-plane problem. *Journal of Modern Optics,* 42.

Ganci, S., 1996. Half-plane diffraction in a case of oblique incidence. *Journal of Modern Optics*, 43.

Guan, Y., Gong, S.X., Zhang, S., Hong, T., 2011. Improved time-domain physical optics for transient scattering analysis of electrically large conducting targets. *IET Microwaves, Antennas and Propagation*, 5.

Hamel, P., Adam, J.P., Kubické, G., Pouliguen, P., 2012. An improved hybridization technique of geometrical optics physical optics.*15th International Symposium on Antenna Technology and Applied Electromagnetics*, Antem.

Huang, K., He, Z.L., Zhang, H.W., Liang, C.H., 2011. Efficient analysis of antenna around electrically large platform with improved non-uniform rational B-spline hybrid method of moments and physical-optics method. *IET Microwaves, Antennas and Propagation*. 5.

Knott, E.F., 1985. The relationship between mitzner's ILDC and michaeli's equivalent currents. *IEEE Trans Antennas Propag*, 33.

Lee, J., Havrilla, M., Hyde, M., Rothwell, E.J., 2008. Scattering from a cylindrical resistive sheet using a modified physical optics current. *IET Microwaves, Antennas and Propagation*, 2.

Letrou, C., Boag, A., 2012. Generalized multilevel physical optics (MLPO) for comprehensive analysis of reflector antennas. *IEEE Trans Antennas Propag*, 60.

Maggi G.A., 1888. Sulla propagazione libre e perturbata delle onde luminose in un mezzo izotropo. *Annals of Mathematics*, 16.

Michaeli A., 1984. Equivalent edge currents for arbitrary aspects of observation. *IEEE Trans. Antennas Propogat*, AP-32.

Mitzner K.M., 1974. Incremental length diffraction coefficients. Aircraft Division Northrop Corp., Tech. Rep. No. AFAL-TR-73-296.

Roudstein, M., Boag, A., 2011. Double-bounce multi-level physical optics algorithm for far-field scattering. IEEE International Conference on Microwaves, Communications, Antennas and Electronic Systems.

Rubinowicz, A., 1957. Thomas Young and the theory of diffraction. *Nature*, 180.

Rubinowicz A., 1917. Die beugungswelle in der Kirchoffschen theorie der beugungsercheinungen. *Annals of Physics*, 4.

Ufimtsev P. Ya., 1971. Method of Edge Waves in the Physical Theory of Diffraction. Air Force Systems Command, Foreign Tech. Div. Document ID No. FTD-HC-23-259-71.

Ufimtsev, P.Y., 2006. Fundamentals of the Physical Theory of Diffraction.

Umul, Y.Z., 2008a. MTPO based potential function of the boundary diffraction wave theory. *Optics & Laser Technology*, 40.

Umul, Y.Z., 2008b. Scattering of a line source by a cylindrical parabolic impedance surface. *Journal of the Optical Society of America A*, 25.

Umul, Y.Z., 2009. Rigorous expressions for the equivalent edge currents. Progress In Electromagnetics Research B.

Wu, S.Z., Zhang, S.Q., Jiang, J.H., Li, Y., Wei, B., 2011. Research on electromagnetic scattering characteristics of electrically large object based on time-domain physical optics. *Proceedings of 2011 Cross Strait Quad-Regional Radio Science and Wireless Technology Conference*, CSQRWC.

Yalçin, U., 2007. Scattering from a cylindrical reflector: modified theory of physical optics solution. *Journal of the Optical Society of America A,* 24.